ACS APPLIED MATERIALS & INTERFACES

Research Article

www.acsami.org

Effect of Gold Nanorods in an MgO Protective Layer of AC Plasma Display Panels

Seok Ho Cho, Seong Min Lee, Woo Hyun Kim, and Kyung Cheol Choi*

Department of Electrical Engineering, Korea Advanced Institute of Science and Technology, Yuseong-gu, Daejeon 305-701, Republic of Korea

Supporting Information

ABSTRACT: We propose a modified MgO protective layer for alternating current plasma display panels. The modified MgO protective layer of the panel tested here has a structure that incorporates silica-coated Au nanorods (NRs), leading to localized surface plasmon resonance (LSPR) in the near-infrared (IR) region. The silica-coated Au NRs were synthesized by a simple chemical method and inserted into an MgO protective layer using an air-spray method. The operating voltage of the proposed structure was decreased by 10 V. The luminance and luminous efficacy of the test panel part with the silica-coated Au NRs both increased by about 15%. According to the measured results of the IR response time, the sustain discharge time lag was reduced. In addition, by inserting the silica-coated Au NRs into the MgO protective layer, a decrease of the IR emission proceeding from the plasma discharge was acquired. Finally, we investigated the LSPR effect of the silica-coated Au NRs in a simulation with a finite-difference time domain method.

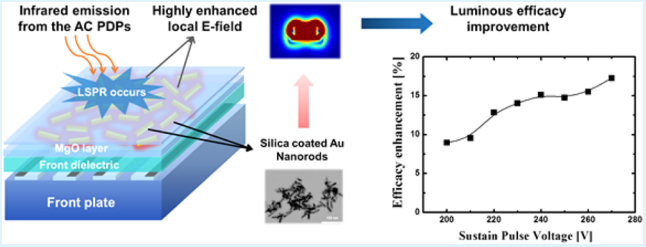

KEYWORDS: *gold nanorods, localized surface plasmon resonance (LSPR), MgO protective layer, alternating current plasma display panels (AC PDPs), silica coating*

1. INTRODUCTION

Alternating current plasma display panels (AC PDPs) have recently become distinguished in the 3D display market. There have been diverse attempts to enhance the luminous efficacy of AC PDPs because these PDPs have relatively low luminous efficacy compared to other flat panel displays.[1−3] In particular, there have been several reports to enhance the luminous efficacy of AC PDPs by changing the material of the protective layer[4−6] and modifying the surface morphology of the protective layer.[7,8] When using these methods, a lower operating voltage and a shorter discharge time are obtained. Also, several applications of localized surface plasmon resonance (LSPR) due to nanoparticles and nanorods (NRs) have recently been reported.[9−11] In our previous report, we improved the luminous efficacy of a test panel through the application of silica-coated Au NRs into an MgO protective layer. However, the effects of silica-coated Au NRs in the MgO protective layer have not been completely identified.[12] This paper identifies an enhancement of the discharge characteristics after inserting silica-coated Au NRs into the MgO protective layer and investigates the reasons behind these phenomena. By inserting the silica-coated Au NRs into the MgO protective layer, a highly enhanced local electric field induced by the LSPR of the silica-coated Au NRs in the near-IR region and a nanoscale rough surface was obtained on the MgO protective layer without transmittance loss through the visible wavelength. The highly enhanced local electric field and the nanoscale rough surface of the MgO protective layer have positive effects on the discharge characteristics of the test panel. In addition, the silica-coated Au NRs absorb infrared (IR) rays because they generate LSPR at the near-IR region.[13,14] The IR emission from the AC PDPs as caused by plasma discharge can interfere with other electronic devices, such as near-IR remote-control devices.[15] Therefore, the decrease of the IR emission from AC PDPs by means of the silica-coated Au NRs is another advantage. To produce LSPR at the IR region, it is necessary to use Au NRs, as Au NRs can easily control the LSPR wavelength from the red light range to IR region due to the plasmon oscillation of electrons along the long axis of the Au NRs.[13] As the length of the long axis increases, the LSPR wavelength moves to a longer wavelength. This is the first trial of the application of LSPR on a protective layer of AC PDPs through the insertion of silica-coated Au NRs into the MgO protective layer.

2. EXPERIMENTAL SECTION

2.1. Synthesis of Au NRs. According to the literature, there is a linear dependence of the LSPR wavelength on the aspect ratio of NRs.[16] LSPR occurs at the near-IR region when the aspect ratio is 4. Therefore, we chose to synthesize the Au NRs with an aspect ratio of 4.

Received: December 21, 2014
Accepted: March 20, 2015
Published: March 20, 2015

DOI: 10.1021/am509009v
ACS Appl. Mater. Interfaces 2015, 7, 7559−7565

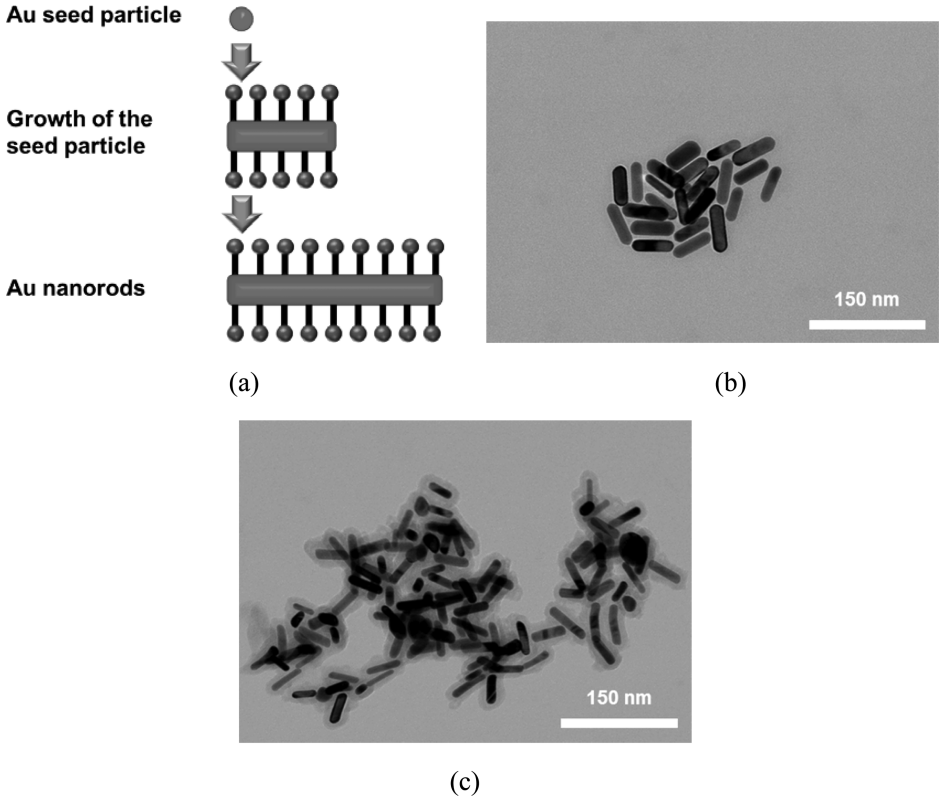

Figure 1. (a) Schematic diagram of the synthesis process of the Au NRs. Scanning transmission electron microscope images of (b) the Au NRs and (c) the silica-coated Au NRs.

Figure 1(a) shows a schematic diagram of the synthesis process of the Au NRs. To synthesize the Au NRs, a simple wet chemistry method (seed-mediated growth method) was used.[17,18] The seed-mediated growth method is made up two stages, and deionized water was used for the solution experiments. The first stage is the synthesis of the Au seed particles and the second stage is the growth of the Au NRs in a growth solution.

2.1.1. Synthesis of the Au Seed Particles. Five milliliters of a 0.2 M solution of hexadecyltrimethylammonium bromide (CTAB, 99%, Sigma- Aldrich) was mixed with 5 mL of an aqueous 0.0005 M solution of hydrogen tetrachloroaurate trihydrate ($HAuCl_4{\cdot}3H_2O$, 99.9%, Sigma- Aldrich). Then, 0.60 mL of an ice-cold aqueous 0.010 M $NaBH_4$ (99%, Sigma- Aldrich) solution was added. Vigorous stirring of the seed solution was then done for 2 min. The color of the seed solution was brownish yellow and the size of the seed particles was less than 4 nm. The size of the seed particles was determined by scanning transmission electron microscope (STEM) measurements. This seed solution was kept at room temperature for later use.

2.1.2. Growth of the Au NRs. Ten milliliters of a 0.2 M solution of CTAB was mixed with 0.5 mL of a 0.0040 M solution of AgNO3 at 25 °C. Then, 10 mL of a 0.0010 M solution of $HAuCl_4{\cdot}3H_2O$ was added. After mixing the solution, 140 μL of a 0.08 M solution of ascorbic acid (99%, Sigma-Aldrich) was added. Ascorbic acid changes the growth solution so that it becomes colorless and transparent. Finally, 30 μL of the seed solution was added to the growth solution at room temperature.

Figure 1(b) shows a STEM image of the synthesized Au NRs. The major axes of the Au NRs range from 50 to 70 nm, the minor axes of the Au NRs range from 15 to 20 nm. The aspect ratios of the Au NRs range from 3 to 4.

2.2. Coating of Silica on CTAB-Capped Au NRs. To deposit the Au NRs on the MgO protective layer, we use an air-spray method. For this spray method, a volatile solvent, such as ethanol, is required to avoid leaving a residue. However, the solvent of the synthesized Au NRs solution is deionized water, meaning that it was necessary to change the solvent of the Au NRs to ethanol. To change the solvent to ethanol, the Au NRs should be coated with silica. Without a silica coating, the Au NRs become aggregated, and their optical properties disappear. In addition, silica is a good generalized platform coating candidate. To coat silica onto the surfaces of Au NRs, a sol gel chemistry method was used.[19] After the elimination of surplus CTAB by centrifuging three times, an amount of 50 mL of the Au NRs solution (for an Au NR concentration about 10^{13}–10^{15} particles/L) was mixed with 90 μL of tetraethyl orthosilicate (TEOS, 99.9%, Sigma-Aldrich). After stirring for a couple of days, mesoporous silica was homogeneously coated onto the Au NRs. We confirmed that the Au NRs were well coated with silica through EDS measurements. Figure 1(c) shows STEM images. As shown in Figure 1(c), the coating thicknesses were approximately 10–15 nm.

Table 1. EDS Measurements Data of the Silica-Coated Au NRs

elements	weight %	atomic %
C	16.70	52.08
O	6.17	14.44
Al	2.30	3.19
Si	6.49	8.65
Cu	21.64	12.76
Au	46.70	8.88
total	100	100

2.3. Fabrication of an MgO Protective Layer with Inserting Silica-Coated Au NRs. To fabricate the MgO protective layer incorporating the silica-coated Au NRs, 480 nm of the first MgO layer was deposited by electron-beam (E-beam) evaporation at 150 °C. Then, the silica-coated Au NRs were deposited on 480 nm of the first MgO layer using an air-spray method. The silica-coated Au NRs were dispersed in ethanol. This solution was sprayed by the air-spray method at room temperature at atmospheric pressure. Ethanol is highly volatile; therefore, soon after the particle solution reached the

DOI: 10.1021/am509009v
ACS Appl. Mater. Interfaces 2015, 7, 7559–7565

MgO layer, the ethanol evaporated, leaving only the silica-coated Au NRs. Twenty nanometers of a second MgO layer was deposited via atomic layer deposition (ALD) at 100 °C. After this process, the proposed MgO protective layer was completed.

Figure 2 presents a scanning electron microscopy (SEM) image of a front plate of the test panel with the MgO protective layer with inserted silica-coated Au NRs. From the SEM image, the silica-coated Au NRs are distributed homogeneously without particle aggregation. The inset in Figure 2 shows a cross-sectional SEM image of the front plate of the test panel with the MgO protective layer with the inserted silica-coated Au NRs. From this image, a nanoscale rough surface of the MgO protective layer is observed without critical damage caused by heat or plasma discharge.

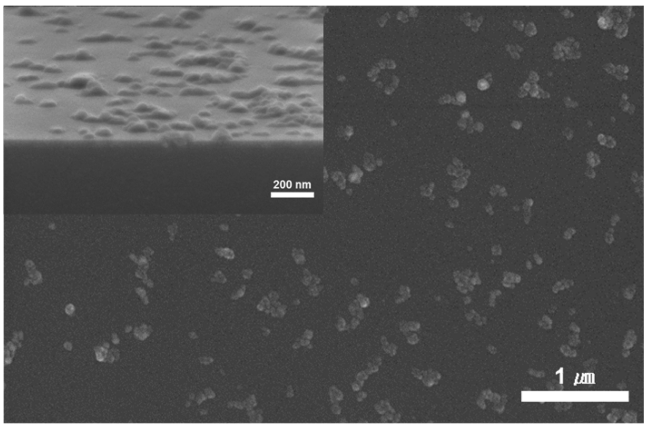

Figure 2. Scanning electron microscopy image of the proposed MgO Protective layer incorporating the silica-coated Au NRs. Inset: Cross sectional scanning electron microscopy image of the proposed MgO Protective layer incorporating the silica-coated Au NRs.

2.4. Test Panel Fabrication and Device Specifications. A 4-in test panel was fabricated to measure the test panel characteristics. The size of each individual cell was 1080 × 360 μm^2, which corresponded to a 42-in VGA resolution panel. The coplanar gap between the common electrodes and the scan electrodes was 80 μm; the width of the ITO sustain electrode was 200 μm, and the width of the Ag bus electrode was 60 μm. A stripe type of barrier rib was used, and the height of the barrier rib was 180 μm. A mixed gas consisting of 96% of Ne and 4% of Xe was used as the discharge gas under 450 Torr.

Figure 3 indicates a schematic diagram of the front plate with the conventional MgO protective layer part and with the proposed MgO protective layer incorporating the silica-coated Au NRs. In particular, the silica-coated Au NRs were sprayed on only half of the test panel. In other words, the test panel consists of the conventional MgO protective layer part and the proposed MgO protective layer part with silica-coated Au NRs inserted into it. This allowed us to compare the discharge characteristics in an identical environment (Figure S1 in the Supporting Information, SI). Lastly, the test panel was sealed at room temperature using an UV-curable sealant (Figure S2 in the SI).

3. RESULTS AND DISCUSSION

Figure 4(a) presents the absorbance spectra of the Au NRs and the silica-coated Au NRs in DI water. Also, Figure 4(b) presents the relative transmittance, which is the ratio of the transmittance of the MgO protective layer with the inserted silica-coated Au NRs (glass substrate/first MgO, 480 nm/silica-coated Au NRs/second MgO, 20 nm) and the transmittance of the conventional MgO protective layer (glass substrate/first MgO, 480 nm/second MgO, 20 nm). The relative transmittance was also measured using a UV−vis spectrometer. As shown in Figure 4(a), the Au NRs have two plasmonic peaks at 530 and 820 nm which originate from the excitation of surface plasmons in directions perpendicular and parallel, respectively, to the major axes of the Au NRs. Also, Figure 4(a) shows that the silica-coated Au NRs absorb the near-IR region by excitation of the LSPR and red-shifted plasmon peaks because the Au NRs were coated with silica, which has a higher refractive index than DI water. The 600 nm absorption peak of the silica-coated Au NRs occurred during the silica-coating process. However, we confirmed that the 600 nm peak of the silica-coated Au NRs is of little importance (Figure S3 in the SI). As shown in Figure 4(b), the relative transmittance at 828 nm of the MgO protective layer incorporating the silica-coated Au NRs is approximately 85%. The MgO protective layer with the silica-coated Au NRs has relatively low relative transmittance at 828 nm because the silica-coated Au NRs absorbed the 828 nm wavelength, which originated from the excitation of the LSPR.

Figure 5 shows the firing voltage, minimum sustain voltage, luminance, the power density, and the luminous efficacy of the test panel part with the conventional MgO protective layer and

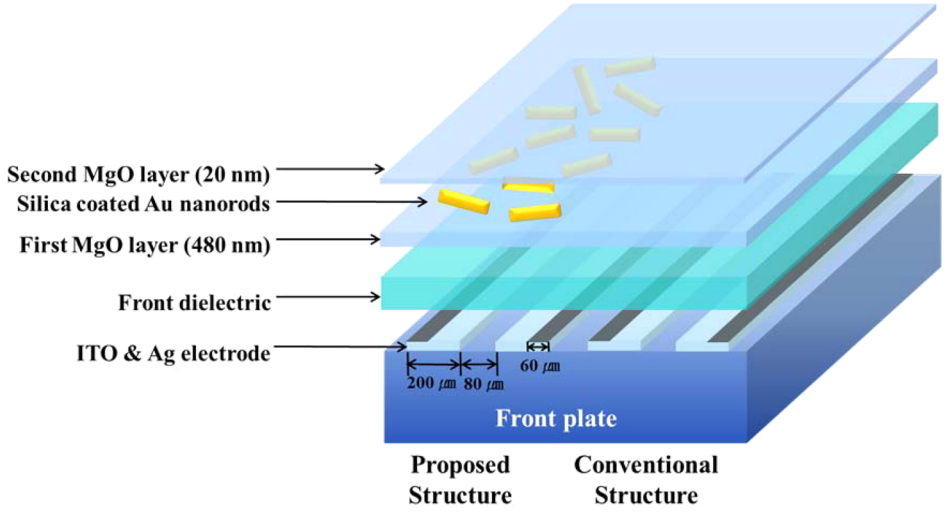

Figure 3. Schematic diagram of a front plate with the conventional MgO layer part and with the proposed MgO layer part with the silica-coated Au NRs.

DOI: 10.1021/am509009v
ACS Appl. Mater. Interfaces 2015, 7, 7559−7565

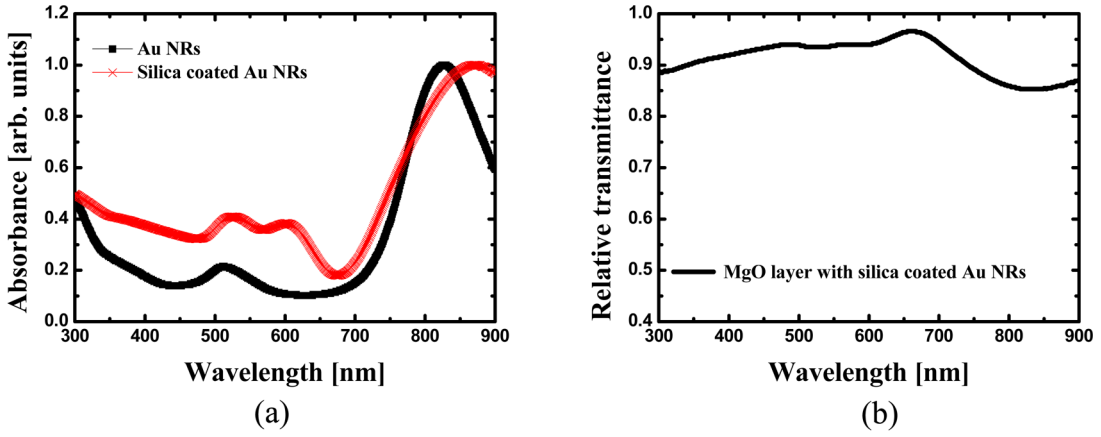

Figure 4. (a) UV−visible absorption spectrum of the Au NRs and the silica-coated Au NRs in DI water and (b) relative transmittance of the MgO protective layer with the inserted silica-coated Au NRs.

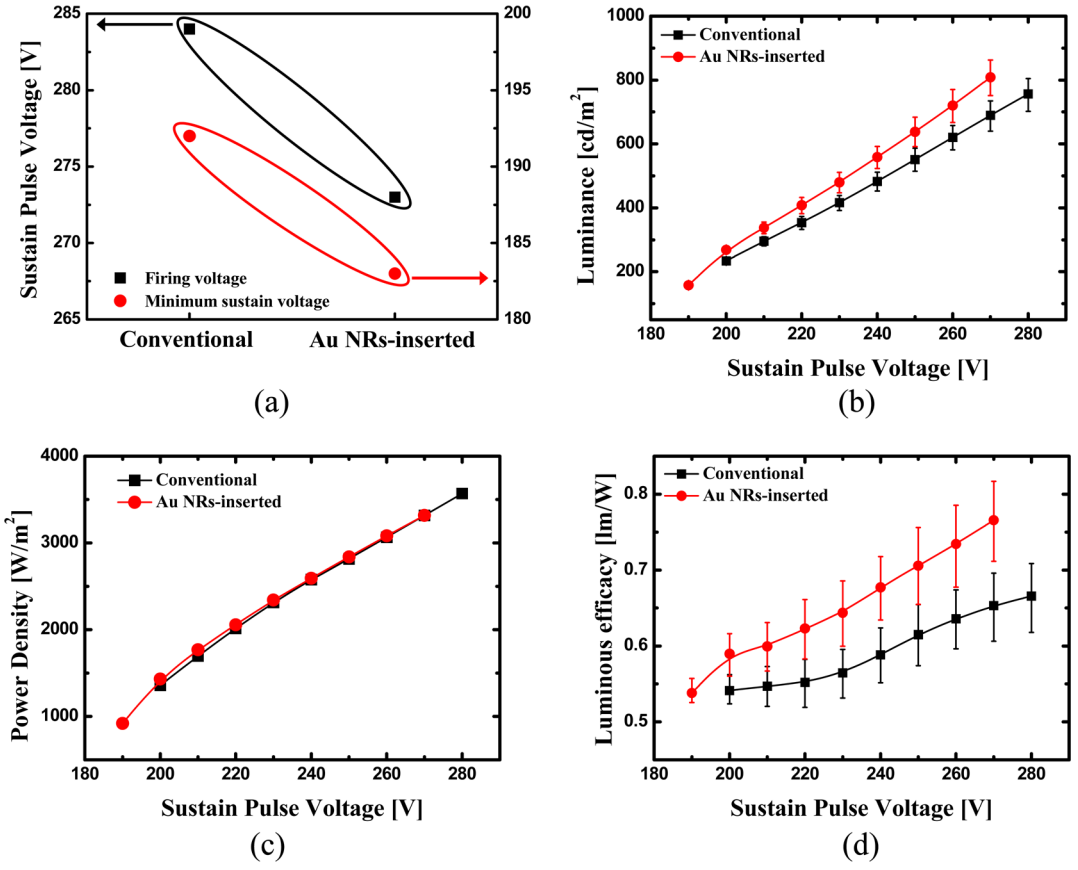

Figure 5. (a) Firing voltage and minimum sustain voltage, (b) luminance, (c) power density, and (d) luminous efficacy of the test panel part with the conventional MgO protective layer and of the test panel part with the proposed MgO protective layer incorporating silica-coated Au NRs.

the test panel part with the proposed MgO protective layer incorporating the silica-coated Au NRs. To measure these data, a sustained square voltage pulse with a frequency of 50 kHz and a width of 4 μs was used. As shown in Figure 5(a), the firing voltage and the minimum sustain voltage of the test panel part with the silica-coated Au NRs decreased by approximately 11 and 12 V, respectively, compared to the test panel part without the silica-coated Au NRs. The firing voltage was measured by gradually increasing the square sustain voltage pulse until the discharge was initiated. Also, the minimum sustain voltage was measured by decreasing the square sustain voltage pulse until the first cell began to turn off.[20] According to the literature, the minimum sustain voltage is related to the wall voltage.[21,22] Therefore, the magnitude of the wall voltage of the test panel part with the silica-coated Au NRs most likely increased. In addition, the static sustain margins of the conventional MgO protective layer part and of the proposed MgO protective layer part with the silica-coated Au NRs were similar. Figure 5(b) shows that the luminance of the test panel part with the proposed MgO protective layer incorporating the silica-coated Au NRs was higher than that of the test panel part with the conventional MgO layer. A green phosphor with an emission peak at 550 nm and an emission spectrum in the wavelength range of 450 to 650 nm was used for the test panel. In addition,

DOI: 10.1021/am509009v
ACS Appl. Mater. Interfaces 2015, 7, 7559−7565

the luminance values were measured with a spectroradiometer (Konica Minolta, CS-1000). We measured the conventional MgO protective layer part and the proposed MgO protective layer part with silica-coated Au NRs at three different points in each case (the left part, the middle part, and the right part). Next, we calculated the average luminance values. The luminance data in Figure 5(b) is an averaged value. The silica-coated Au NRs rarely absorb visible light emissions from phosphor, as shown in Figure 4(b). Therefore, the silica-coated Au NRs did not have a detrimental effect on the luminance. The power density of the test panel part with the proposed MgO layer incorporating the silica-coated Au NRs was slightly higher than that of the test panel part with the conventional MgO layer, as shown in Figure 5(c). The power consumption of the test panel was measured by deducting the power consumed by an off-state test panel from the power consumed of an on-state test panel. The luminous efficacy was obtained by the ratio of the luminance and the power consumption data of the test panel. From Figure 5(d), the luminous efficacy of the test panel part with the proposed MgO layer incorporating the silica-coated Au NRs was higher than that of the test panel part with the conventional MgO protective layer. The luminous efficacy of the test panel part with the silica-coated Au NRs was enhanced by about 15% compared to the test panel part with the conventional MgO protective layer. There are several reasons for the enhanced performance of the test panel part with silica-coated Au NRs inserted into it. The nonflattened surface morphology of the MgO protective layer and the LSPR in the IR region induce a highly enhanced local electric field. In particular, the nonflattened surface morphology of the MgO protective layer is expected to enhance the secondary electron emission (SEE).[23] In addition, according to previous work by our group, the work function of an MgO protective layer incorporating gold nanoparticles is lower than that of a conventional MgO protective layer.[7] We therefore believe that the work function of the MgO protective layer incorporating Au NRs is also lower than that of the conventional MgO protective layer. Moreover, when the Au NRs are inserted, the SEE is enhanced accordingly.[6] Also, the ion bombardment incident angle was changed, and the surface area of the MgO protecting layer was increased after the insertion of the silica-coated Au NRs. These changes have the potential to enhance the discharge characteristics of the test panel part with silica-coated Au NRs inserted into it.

Figure 6 indicates the IR response time of the test panel part with the conventional MgO protective layer and of the test panel part with the proposed MgO protective layer incorporating the silica-coated Au NRs. The IR emission from the test panel has a wavelength of 828 nm, and it originates from the relaxation of Xe from a higher excited state to a lower excited state. The IR response time is defined as the time difference between the 10% level of the peak voltage and the 10% level of the peak IR value.[20] The IR value was measured with a photodetector (Hamamatsu, C6386). The response time of the MgO protective layer after inserting the silica-coated Au NRs decreased compared to that of the conventional MgO protective layer. The IR response time is affected by the intensity of the electric field on the discharged cell.[7,20] Accordingly, we believe that the total intensity of the electric field on the discharged cell of the MgO protective layer with the silica-coated Au NRs was greater than that of the MgO protective layer without the silica-coated Au NRs because an enhanced local electric field induced by the LSPR of the silica-coated Au NRs in the near-IR region and the nanoscale rough surface of the MgO protective layer was added. This enhanced local electric field can lead to enhanced discharge characteristics compared to the conventional MgO protective layer.

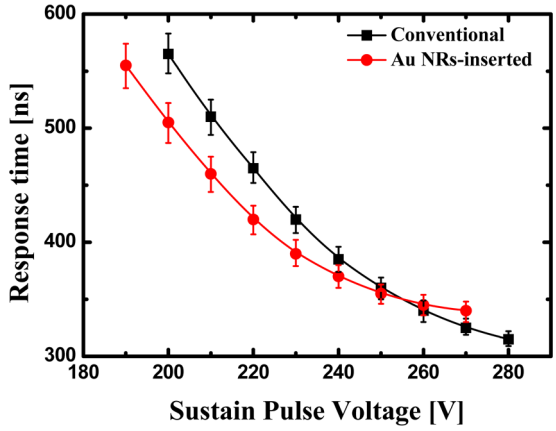

Figure 6. IR response time of the test panel part with the conventional MgO protective layer and of the test panel with the MgO protective layer incorporating the silica-coated Au NRs.

Figure 7 presents the IR intensity of the test panel part with the conventional MgO protective layer and the test panel part with the MgO protective layer with the inserted silica-coated Au NRs. The IR intensity was determined by integrating the value of the temporal IR emission, while the IR emission was measured with the photodetector. In the test panel part with the silica-coated Au NRs, the IR intensity was decreased by approximately 7% at the same sustain voltage. However, arithmetically, the rate of the decrease of the IR intensity should have been 15%, as the transmittance at 828 nm of the front plate with the silica-coated Au NRs was approximately 85%, as shown in Figure 4(b). The reason why the rate of the decrease of the IR intensity of the test panel part with the silica-coated Au NRs was only 7% stems from the improvement of the discharge characteristics after inserting the silica-coated Au NRs into the MgO protective layer. The IR emission proceeding from the plasma discharge of AC PDPs can interfere with other electronic devices, such as near-IR remote-control devices. Consequently, an optical filter that blocks the

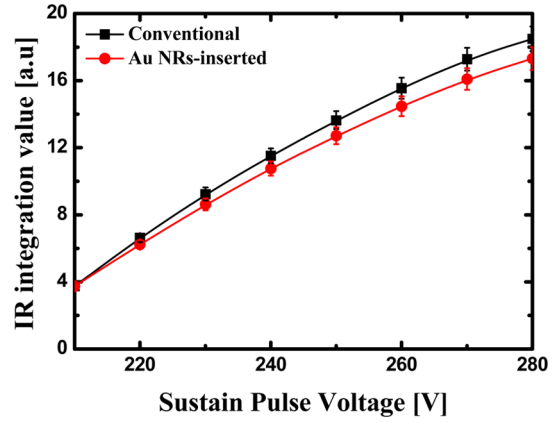

Figure 7. Integration values of the IR emission of the test panel part with the conventional MgO protective layer and of the test panel part with the proposed MgO protective layer incorporating silica-coated Au NRs.

DOI: 10.1021/am509009v
ACS Appl. Mater. Interfaces 2015, 7, 7559−7565

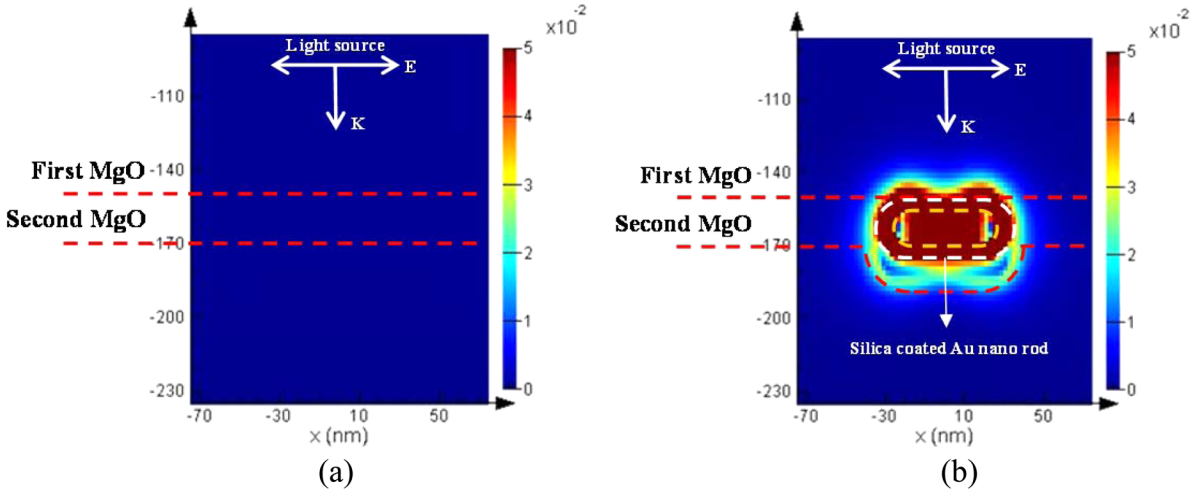

Figure 8. Simulated electric field profile for (a) the conventional MgO protective layer, (b) the proposed MgO protective layer with the inserted silica-coated Au NRs exposed to IR at a wavelength of 828 nm.

near-IR region is used to avoid interference with other electronic products.[15] However, the optical filter has a side effect in that it slightly decreases the transmittance in the visible region. Therefore, the decrease of the IR intensity after the insertion of the silica-coated Au NRs into the MgO protective layer can relieve this side effect of the optical filter.

We finally investigated the LSPR effect of the silica-coated Au NRs in a simulation with a finite-difference time domain (FDTD) method to explain the enhanced local electric field (Figure S4 in the SI). From our STEM images in Figure 1, the major axis of the Au NR was estimated to be 60 nm, the minor axis of the Au NR was approximately 16 nm, and the silica thickness of the silica-coated Au NRs was 10 nm. The light source is a plane wave that comes through the semi-infinite substrate with propagation vector k vertical to the surface, and the electric field of the light source E is polarized parallel to the surface. The intensity of the incident light source is 1. The optical constants (n, k) of the MgO protective layer were measured by an ellipsometric measurement method and were used as the input parameters in the FDTD simulator. Figure 8, parts (a) and (b), show the simulated electric field profile in the conventional MgO protective layer and the proposed MgO protective layer at a wavelength of 828 nm. From Figure 8(b), we confirmed the excitation of the LSPR and the enhanced local electric field in the vicinity of the silica-coated Au NRs. The strong localized electric field induced by the LSPR of the Au NRs contributed to the decrease of the IR response time, thus explaining the enhancement of the discharge characteristics. In contrast, there was no significant enhancement of the electric field in the conventional MgO protective layer, as shown in Figure 8(a).

4. CONCLUSIONS

Here, Au NRs were synthesized using a seed-mediated growth method and were coated with silica using a sol gel chemistry method. Subsequently, the silica-coated Au NRs were deposited onto the MgO protective layer using an air-spray method. A highly enhanced local electric field induced by the LSPR of the silica-coated Au NRs in the near-IR region and a nanoscale rough surface of the MgO protective layer were obtained by inserting the silica-coated Au NRs into the MgO protective layer. These changes improve the discharge characteristics of AC PDPs. Consequently, a test panel part with the silica-coated Au NRs achieved a lower operating voltage, higher luminous efficacy, and a shorter IR response time than a conventional test panel part. In addition, the silica-coated Au NRs absorb IR rays because they create LSPR in the near-IR region, after which a decrease of the IR emission is acquired. The effects of the LSPR of the silica-coated Au NRs, including an enhanced local electric field in the near-IR region, were confirmed in a simulation using the FDTD method.

The present work shows that the luminous efficacy of AC PDPs can be enhanced by inserting silica-coated Au NRs into the MgO protective layer without additional complex fabrication processing or expensive fabrication processes.

■ ASSOCIATED CONTENT

Supporting Information

Image of the fabricated test panel, FDTD simulated electric field profiles of the MgO protective layer with the silica-coated Au NRs, and the extinction spectrum of the MgO protective layer with the silica-coated Au NRs. This material is available free of charge via the Internet at http://pubs.acs.org.

■ AUTHOR INFORMATION

Corresponding Author

*Phone: +82-42-350-3482; fax: +82-42-350-8082; e-mail: kyungcc@kaist.ac.kr (K.C.C.).

Author Contributions

S.H.C. and K.C.C. conceived and designed the experiments and prepared the manuscript. S.H.C. synthesized the gold nanorods, fabricated the test panel, and performed the FDTD simulation. S.H.C., S.M.L., and W.H.K. measured the test panel. All authors discussed the results and commented on the manuscript.

Notes

The authors declare no competing financial interest.

■ ACKNOWLEDGMENTS

This research was supported by Basic Science Research Program through the National Research Foundation of Korea (NRF) funded by the Ministry of Education, Science and Technology (CAFDC-20120000820).

DOI: 10.1021/am509009v
ACS Appl. Mater. Interfaces 2015, 7, 7559−7565

ABBREVIATIONS

AC PDPs, alternating current plasma display panels
LSPR, localized surface plasmon resonance
NRs, nanorods
IR, infrared
STEM, scanning transmission electron microscope
E-beam, electron-beam
ALD, atomic layer deposition
SEM, scanning electron microscopy
SEE, secondary electron emission
FDTD, finite difference time domain

REFERENCES

(1) Oversluizen, G.; Klein, M.; de Zwart, S.; van Heusden, S.; Dekker, T. Improvement of the Discharge Efficiency in Plasma Displays. *J. Appl. Phys.* **2002**, *91*, 2403−2408.

(2) Choi, K. C.; Shin, N. H.; Song, S. C.; Lee, J. H.; Park, S. D. A New AC Plasma Display Panel with Auxiliary Electrode for High Luminous Efficacy. *IEEE Trans. Electron Devices* **2007**, *54*, 210−218.

(3) Lee, S. M.; Kim, Y. K.; Kim, M. K.; Park, H. B.; Choi, K. C. Nanoplasmon-Enhanced Light Emitter for AC Plasma Display Panels with Large Scalability. *IEEE Trans. Electron Devices* **2012**, *59*, 2727−2734.

(4) Whang, K. W.; Jung, H. Y.; Lee, T. H.; Kwon, O.; Cheng, H. W.; Stein müller, S. O.; Janek, J. High Luminous Efficacy and Low Driving Voltage PDP with SrO-MgO Double Protective Layer. *IEEE Electron Device Lett.* **2010**, *31*, 686−688.

(5) Kim, R. H.; Kim, Y. H.; Park, J. W. Electrical Properties of Evaporated MgO-TiO_2 Protective Layer for AC PDP. *J. Mater. Sci.* **2001**, *36*, 1496−1473.

(6) Motoyama, Y.; Murakami, Y.; Seki, M.; Kurauchi, T.; Kikuchi, N. SrCaO Protective Layer for High-Efficiency PDPs. *IEEE Trans. Electron Devices* **2007**, *54*, 1308−1314.

(7) Kim, W. H.; Cho, K. H.; Choi, K. C. Influence of Gold Nanoparticles on the Characteristics of Plasma Display Panels. *IEEE Trans. Electron Devices* **2010**, *57*, 2644−2650.

(8) Cho, K. H.; Ahn, S. I.; Lee, S. M.; Choi, K. C. The Effect of Disordered Microscale Holes in the Front Dielectric Layer of AC Plasma Display Panels. *IEEE Trans. Electron Devices* **2010**, *57*, 2183−2189.

(9) Lee, S. M.; Choi, K. C. Enhanced Emission from $BaMgAl_{10}O_{17}:Eu^{2+}$ by Localized Surface Plasmon Resonance of Silver Particles. *Opt. Express* **2010**, *18*, 12144−12152.

(10) Lee, S. M.; Choi, K. C.; Kim, D. H.; Jeon, D. Y. Localized Surface Plasmon Enhanced Cathodoluminescence from Eu^{3+}-Doped Phosphor Near the Nanoscaled Silver Particles. *Opt. Express* **2011**, *19*, 13209−13217.

(11) Lee, S. M.; Kim, D. H.; Jeon, D. Y.; Choi, K. C. Nanoplasmon-Enhanced Transparent Plasma Display Devices. *Small* **2012**, *8*, 1350−1354.

(12) Cho, S. H.; Kim, W. H.; Lee, S. M.; Choi, K. C. AC Plasma Displays with Gold Nanorods in the Protecting Layer. *SID Int. Symp. Dig. Technol. Pap.* **2012**, *43*, 68−70.

(13) Maier, S. A. *Plasmonics: Fundamentals and Applications*; Springer Verlag: Berlin, 2007.

(14) Hutter, E.; Fendler, J. H. Exploitation of Localized Surface Plasmon Resonance. *Adv. Mater.* **2004**, *16*, 1685−1706.

(15) Song, I. H.; Rhee, C. H.; Park, S. H.; Lee, S. L.; Grudinin, D.; Song, K. H.; Choe, J. H. Continuous Production of a Near Infrared Absorbing Chromophore. *Org. Process Res. Dev.* **2008**, *12*, 1012−1015.

(16) Jain, P. K.; Lee, K. S.; El-Sayed, I. H.; El-Sayed, M. A. Calculated Absorption and Scattering Properties of Gold Nanoparticles of Different Size, Shape, and Composition: Applications in Biological Imaging and Biomedicine. *J. Phys. Chem. B* **2006**, *110*, 7238−7248.

(17) Nikoobakht, B.; El-Sayed, M. A. Preparation and Growth Mechanism of Gold Nanorods (NRs) Using Seed-Mediated Growth Method. *Chem. Mater.* **2003**, *15*, 1957−1962.

(18) Sau, T. K.; Murphy, C. J. Seeded High Yield Synthesis of Short Au Nanorods in Aqueous Solution. *Langmuir* **2004**, *20*, 6414−6420.

(19) Gorelikov, I.; Matsuura, N. Single-Step Coating of Mesoporous Silica on Cetyltrimethyl Ammonium Bromide-Capped Nanoparticles. *NANO Lett.* **2008**, *8*, 369−373.

(20) Son, S. H.; Park, Y. S.; Bae, S. C.; Choi, S. Y. Application of Hollow Channel between Sustain Electrodes to Improve Discharge Characteristics in Alternating Current Plasma Display Panels. *Appl. Phys. Lett.* **2002**, *80*, 1719−1721.

(21) Cho, K. H.; Lee, S. M.; Choi, K. C. Wall Voltage and Priming Effect due to Auxiliary Electrode in AC PDP with Auxiliary Electrode. *IEEE Trans. Plasma Sci.* **2007**, *35*, 1567−1573.

(22) Shin, B. J.; Choi, K. C.; Tae, H. S.; Seo, J. H.; Kim, J. Y.; Han, J. W. Case Studies on Temperature-Dependent Characteristics in AC PDPs. *IEEE Trans. Plasma Sci.* **2005**, *33*, 162−168.

(23) Oh, J. S.; Choi, E. H. Ion-Induced Secondary Electron Emission Coefficient (γ) from MgO Protective Layer with Microscopic Surface Structures in Alternating Current Plasma Display Panels. *Jpn. J. Appl. Phys.* **2004**, *43*, 1154−1155.

DOI: 10.1021/am509009v
ACS Appl. Mater. Interfaces 2015, 7, 7559−7565